Original Article | Journal of Biosystems Engineering

J. of Biosystems Eng. 40(4):335-344. (2015. 12)
http://dx.doi.org/10.5307/JBE.2015.40.4.335

eISSN : 2234-1862
pISSN : 1738-1266

Detecting Drought Stress in Soybean Plants Using Hyperspectral Fluorescence Imaging

Changyeun Mo[1], Moon S. Kim[2], Giyoung Kim[1], Eun Ju Cheong[3], Jinyoung Yang[4], Jongguk Lim[1]*

[1]*National Institute of Agricultural Sciences, Rural Development Administration, Jeonju 54875, Republic of Korea*
[2]*Environmental Microbiology and Food Safety Laboratory, Agricultural Research Service, US Department of Agriculture, MD 20705, USA*
[3]*Division of Forest Sciences, College of Forest and Environment Sciences, Kangwon National University, Chuncheon 24341, Republic of Korea*
[4]*Crop Systems and Global Change Laboratory, Agricultural Research Service, US Department of Agriculture, MD 20705, USA*

Received: November 5th, 2015; Revised: November 12nd, 2015; Accepted: November 19th, 2015

Abstract

Purpose: Soybean growth is adversely affected by environmental stresses such as drought, extreme temperatures, and nutrient deficiency. The objective of this study was to develop a method for rapid measurement of drought stress in soybean plants using a hyperspectral fluorescence imaging technique. **Methods:** Hyperspectral fluorescence images were obtained using UV-A light with 365 nm excitation. Two soybean cultivars under drought stress were analyzed. A partial least square regression (PLSR) model was used to predict drought stress in soybeans. **Results:** Partial least square (PLS) images were obtained for the two soybean cultivars using the results of the developed model during the period of drought stress treatment. Analysis of the PLS images showed that the accuracy of drought stress discrimination in the two cultivars was 0.973 for an 8-day treatment group and 0.969 for a 6-day treatment group. **Conclusions:** These results validate the use of hyperspectral fluorescence images for assessing drought stress in soybeans.

Keywords: Detection, Drought stress, Fluorescence, Imaging, Soybean plant

Introduction

Global food security is of deep concern because of climate change, rapid human population growth, and reduced arable land around the world (Rahaman et al., 2015). In the USA in 2012, 87% of soybean and corn arable lands were affected by drought, causing soybean and corn production to plummet by 25~30%; in turn, this caused an increase in global market prices for the crops. Environmental stresses on crops have intensified because of an increased frequency of factors such as drought and heat wave, which induce abnormal physiological reactions in crops that result in growth inhibition, reduced production, or even plant death. One possible solution to these problems is the development of robust drought tolerant cultivars (Chang et al., 2011).

Although a variety of breeding technologies are available, quantitative measurements of target factors in developed cultivars under different growth environments are difficult using these methods as they are generally very labor-intensive. Recently, to overcome this limitation, several studies have analyzed the relationship between genetic factors and environments by measuring the phenotypic features of growth over time using imaging and spectroscopic measurement technologies. Plant phenomics is the study of phenotypes using physiological and biochemical characteristics of plants, often through use of

***Corresponding author:** Jongguk Lim
Tel: +82-63-238-4117; **Fax:** +82-63-238-4105
E-mail: limjg@korea.kr

novel technologies. Such new technologies enable information on growth characteristics such as color, length, leaf area, moisture contents, and chloroplast conditions to be measured nondestructively (Houle et al., 2010).

A wide array of technologies can be used to obtain biometric information from plants in a non-destructive manner, for example, color imaging, fluorescence imaging, thermal imaging, near-infrared (NIR) imaging, and hyperspectral imaging (Nguyen et al., 2006; Manickavasagan et al., 2008; Duan et al., 2011; Shibayama et al., 2011; Rousseau et al., 2013). Chlorophyll fluorescence imaging has been employed to detect water stress in soybean, maize, wheat, strawberry, and Arabidopsis. In soybean, water stress responses have been monitored using red to far-red fluorescence ratio induced by UV light excitation at 420 nm (Caires et al., 2010). Likewise, chlorophyll fluorescence has been used to evaluate drought responses in Arabidopsis (Woo et al., 2008). Dahn et al. (1992) used laser excitation at 355 nm to generate a chlorophyll fluorescence ratio (F690/F735) that is related to drought stress in maize and wheat plants.

Hyperspectral fluorescence imaging (HSFI) technology is a new spectroscopic technique that simultaneously acquires spectral and image information from each pixel unit of a target object or image for each wavelength. The HSFI technique can be used to analyze components in the leaf surfaces of plants or fluorescence expressed in plants (Kim et al., 2001).

In this study, we used hyperspectral fluorescence imaging with 365 nm UV-A excitation and a partial least square regression (PLSR) model to obtain rapid measurements of the drought stress in soybeans. In addition, prediction periods of drought stress in soybeans using the developed models were investigated.

Materials and Methods

Materials

In the present study, we used two soybean cultivars, William 82 (Cultivar I) and Houjaku Kuwazu (Cultivar II), to examine the effects of drought stress. Seeds for each cultivar were obtained from the Soybean Germplasm Collection Laboratory in USDA-ARS, which is affiliated with the U.S. National Plant Germplasm System. The Houjaku Kuwazu cultivar is a robust drought-tolerant cultivar; the William 82 cultivar is a high-yielding cultivar that is cultivated in the USA. Twenty seeds from each cultivar were germinated for one week, and seedlings were grown for three weeks in a growth chamber at 25°C, with 60% relative humidity, and a daily cycle of 15 h with a light intensity of 600 $\mu molm^{-2}s^{-1}$ and 9 h of dark. Water was supplied once per day. After three weeks, the plants from each cultivar were separated into two groups: a control group that was supplied daily with water; and a drought stress group that did not receive water. To measure the effect of drought stress, hyperspectral fluorescence images were obtained from three plants of each control and treatment group after 2, 4, 6, 8, 10, 14, and 16 days at a two- or four-day interval. In order to consider only stress under the same growth conditions, the third branch from the root of plants with three leaves was excised. To minimize the impact of leaf removal, the petiole of the excised leaves was sealed with 0.06% agar to prevent water evaporation. Hyperspectral fluorescence images of the leaves were obtained within 10 minutes after excision. The same plants were used again in the experiment with a minimum of six days between sampling, thereby providing fluorescence image data from three sample groups with each treatment, i.e., (i) 2, 8, and 16 days, (ii) 4 and 10 days, and (iii) 6 and 14 days. The soil moisture contents in the control and drought stressed group after 16 days were 69.5~75.5% relative humidity (RH) and 1.4~4.4% RH for Cultivar I, respectively, and 68.1~76.1% RH and 1.7~4.0% RH for Cultivar II, respectively.

Hyperspectral imaging system

The hyperspectral fluorescence imaging technique developed by the USDA Agricultural Research Service was used in this study (Figure 1). This system employs a highly sensitive electron multiplying charge-coupled device (EMCCD, MegaLuca R, ANDOR Technology, South Windsor, CT, USA) to acquire hyperspectral fluorescence images. The EMCCD device has an 8 × 8 μm pixel size, is cooled to -20°C by thermoelectric cooling, and sends 14-bit images at a speed of 12.5 MHz. An imaging spectrograph (VNIR Concentric Imaging Spectrograph, Headwall Photonics, Fitchburg, Massachusetts) and C mount lens (F1.9, 35 mm Compact Lens, Schneider Optics, Hauppauge, NY, USA) were fixed in front of the EMCCD. The field of view (FOV) of the images is limited by the slit size, which was set at 25 μm in this study. The line scan image acquired through the slit was spectrally radiated on the EMCCD surface through a diffraction grating; in this way, hyperspectral images

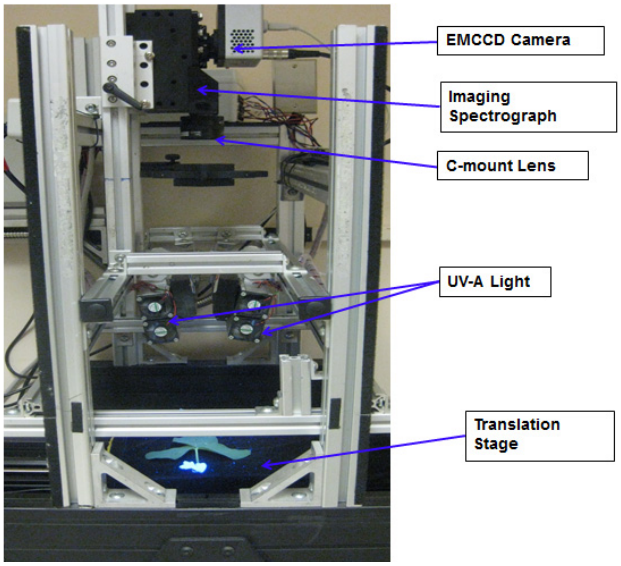

Figure 1. The hyperspectral fluorescence imaging system.

were acquired for each wavelength bandwidth by summing the spectral radiations. Each line scan image therefore had spatial information horizontally and spectrum information vertically.

The light source consisted of four 10 W LED lights that emitted at a wavelength of 365 nm (i.e. UV-A). Two of the light sources were vertically tilted at 15° to excite the samples with the UV-A light. For the hyperspectral fluorescence images, 81 wavelength bands were measured in the wavelength range of 421~780 nm at intervals of 4.8 nm.

Acquiring the hyperspectral image spectrum

In this study, samples of soybean leaves were fixed at the translation stage. Line scan images were obtained with 3 ms exposure time and 1 mm moving steps; 600 lines were measured. Three samples from the same treatment groups of each cultivar were measured simultaneously. In fluorescence images from dark-adapted leaves, the early and middle parts of line-scan of a leaf have different light exposure times; as a result, fluorescence in the middle part of the line-scan may be decreased compared to that in the early part. Therefore, the fluorescence images used here were obtained from leaves after 5 minutes light adaptation to exclude the influence of light exposure time on changes in fluorescence. Dark reference plate images, unexposed to a light source, were measured and fluorescence reference plate images were obtained from a plate where fluorescence was uniformly displayed. The fluorescence reference plate was premium white inkjet paper (Union Camp Co.) that exhibited uniform blue fluorescence (Kim et al., 2001).

The hyperspectral fluorescence images of the sample were corrected using the fluorescence reference plate images (to correct the intensity of fluorescence in the pixels of measured lines) and the dark reference plate images (to compensate for device noise). The corrected fluorescence images of soybean leaves were then converted using the following equation:

$$I(i) = (I_s(i) - D(i))/(I_f(i) - I_d(i)) \quad (1)$$

where, I = corrected relative fluorescence image at the i^{th} wavelength
I_s = sample hyperspectral fluorescence image at the i^{th} wavelength
I_f = hyperspectral fluorescence image of fluorescence plate at the i^{th} wavelength
I_d = hyperspectral image of dark reference at the i^{th} wavelength

Only a soybean leaf part was extracted from the corrected hyperspectral fluorescence image of soybean leaf for acquiring the pixel spectrum and a mean value spectrum of the pixels. Nine mean spectra from three leaves of three different samples were obtained at each sampling interval in the drought stress treatment group and in the control group.

We developed a prediction model to evaluate drought stress in soybeans based on a partial least squares regression (PLSR) analysis. This model used the mean spectrum from leaves of each soybean cultivar during the drought stress treatment period. The values of drought stress treatment and non-treatment were set to "1" and "0," respectively. The prediction model was verified using a cross-validation method and the performance of the model was evaluated using the coefficient of determination (R^2), the root mean square error of calibration (RMSEC), and the root mean square error of validation (RMSEV).

Partial least square (PLS) images were used to verify the developed prediction model. PLS images were obtained by applying the PLSR model to hyperspectral fluorescence images of soybean leaves. Drought stress in the soybeans was identified using a pixel prediction value and mean prediction value derived from the PLS images. The PLS images consist of prediction values calculated by applying regression coefficients, which are weighted for each

wavelength of the PLSR model for all pixel spectra, as expressed in the following equation:

$$\text{PLS Image} = \sum_{i=1}^{n} I_i R_i + C \quad (2)$$

where, I_i = i^{th} image of n spectral images
R_i = regression coefficients of the PLSR model
C = constant of the PLSR model

The prediction accuracy from the PLS image was calculated using the optimum value from the distribution of PLS prediction values of pixels in non-treatment and treatment groups. The overall prediction accuracy was calculated using total accuracies of drought stress treatment and non-treatment groups, and sensitivity and specificity were calculated using predictive accuracies of drought stress treatment and non-treatment groups.

MATLAB (version 7.0.4, Mathworks, Natick, MA, USA) was used to perform data extraction and image data analysis of the acquired hyperspectral fluorescence image spectrum. PLSR model development and validation were carried out using Unscrambler v9.2 data analysis software (CAMO, Oslo, Norway).

Results and Discussion

Spectral characteristics of soybean leaves

As described above, soybean plants from two cultivars were cultivated for 21 days and then assigned to two groups, one of which was then grown under drought stress and the other that was grown under normal conditions and acted as a control. Leaf samples at different times of treatment were obtained using the third branch with

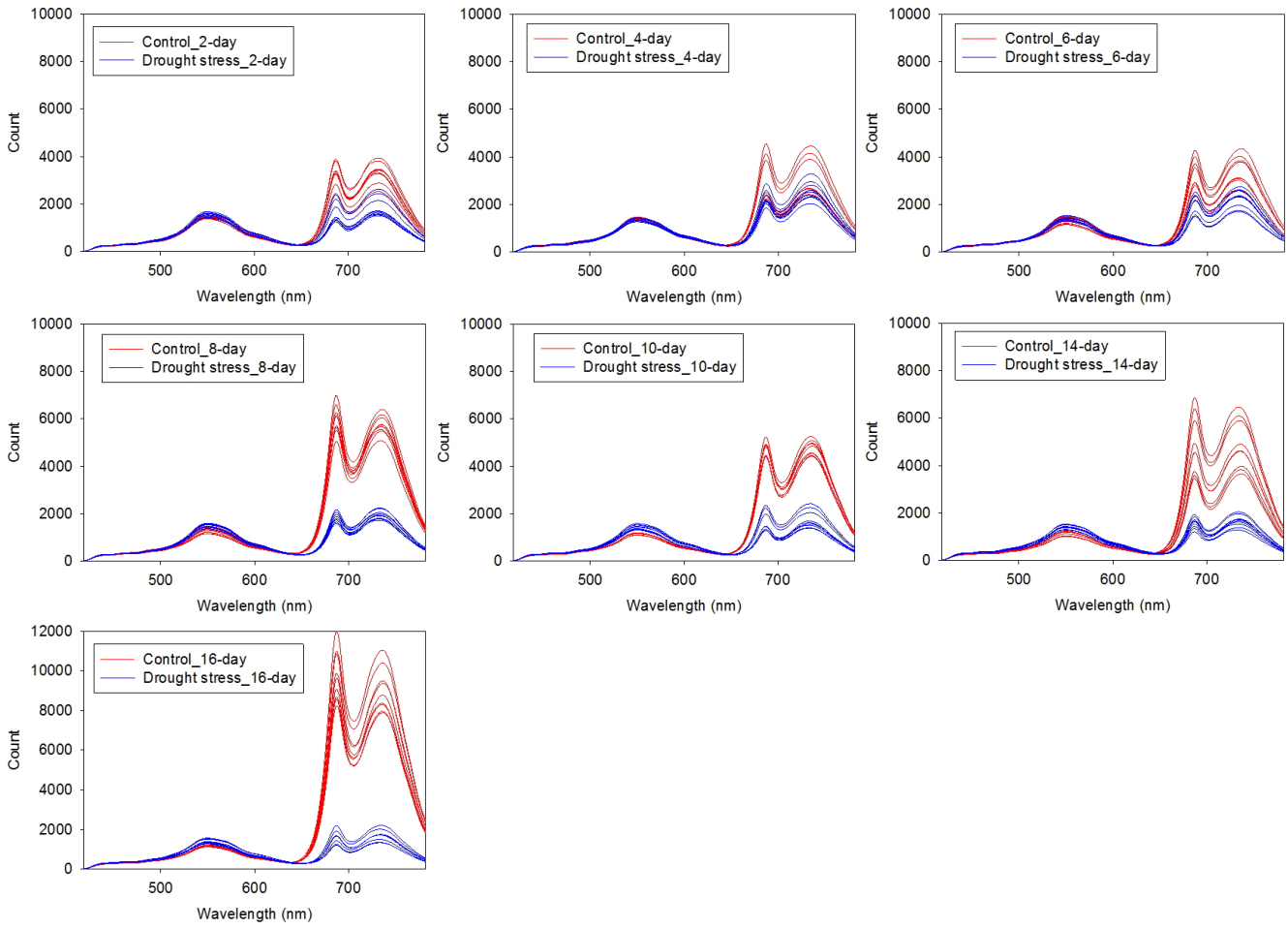

(a)

Figure 2. Average fluorescence spectra of extracted leaves from control and drought stress treated plants from two soybean cultivars: (a) Cultivar I, (b) Cultivar II.

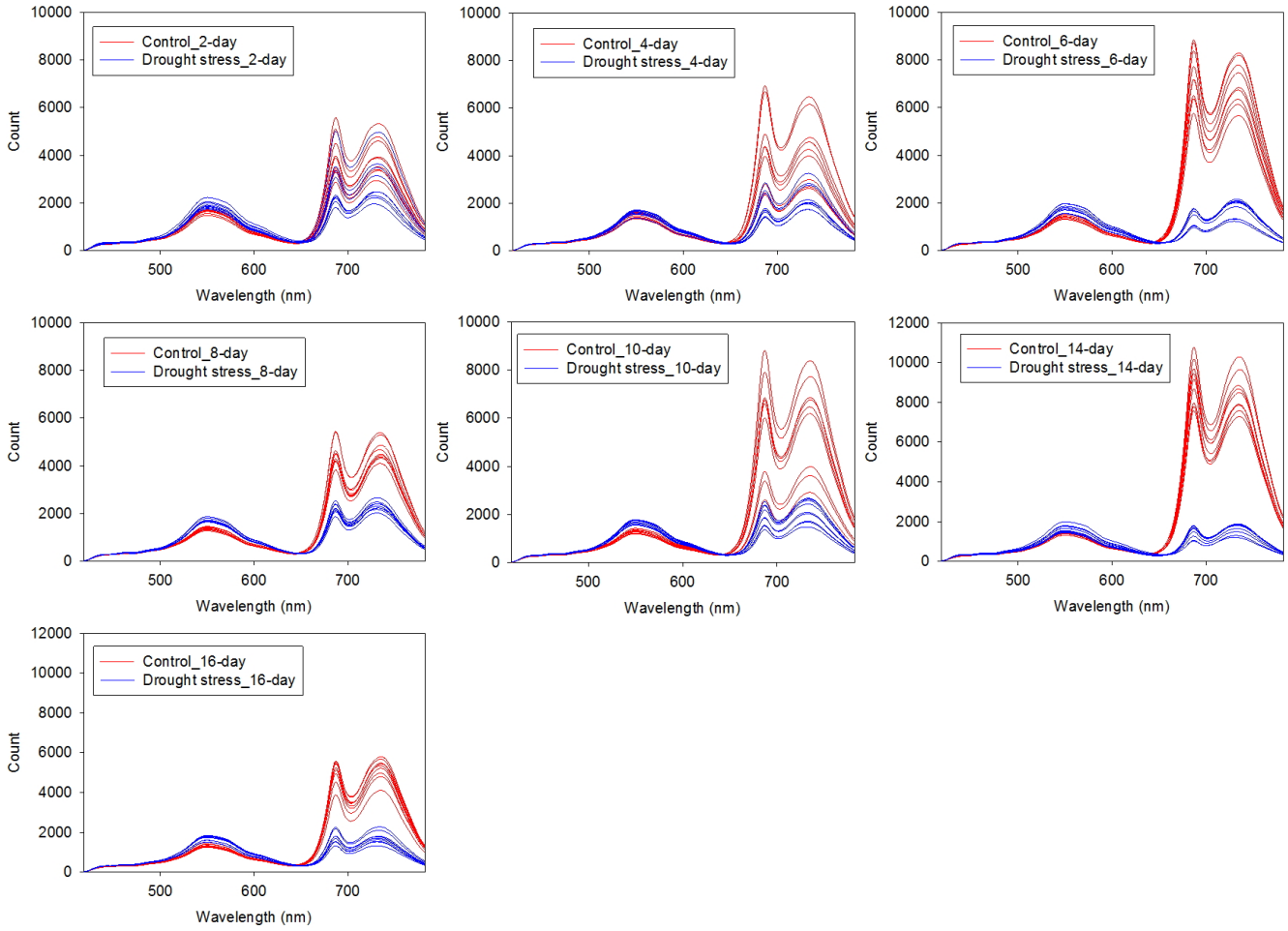

(b)

Figure 2. Average fluorescence spectra of extracted leaves from control and drought stress treated plants from two soybean cultivars: (a) Cultivar I, (b) Cultivar II (Continue).

three leaves from the soil surface. The fluorescence spectra of control and drought stress plants at each sampling interval are shown in Figure 2. In the results, the wavelengths of the fluorescence peaks were 550, 660, and 730 nm for the green, red, and far-red bands, respectively. These bands are related to the wavelengths that display chlorophyll *a* characteristics (Gross, 1991). In both cultivars, the drought stress-treated plants showed a reduction in the difference in fluorescence spectrum between leaves with time, in contrast to the control group. In contrast, control plants showed increased fluorescence intensity with time whereas the stress treated plants tended to show reduced or similar fluorescence intensities. The results here are comparable to those reported in a previous, study wherein it was found that total chlorophyll contents and chlorophyll *a* contents are reduced by increased moisture stress (Buschmann et al., 1998).

PLSR prediction model of drought stress

A PLSR prediction model was developed to assess the relative effects of drought stress in the two soybean cultivars. The results from the drought stress prediction model using the mean spectrum of hyperspectral images of leaves at each sample point are presented Table 1.

The analysis of plants from Cultivar I showed that the prediction model indicated that the 10-day sample had the lowest error among the different drought stress treatment periods. The results with cross-validation of this prediction model showed that R^2 and RMSEV were 0.989 and 0.055, respectively, when the optimum number of factors was 4. At the 8-day interval, the prediction model gave an R^2 of 0.970 and RMSEV of 0.091; although these prediction errors were higher than for the 10-day plants, the optimum number of factors was lower at 1. As the drought stress period increased, the performance of

the prediction model improved in terms of reduction of the optimum number of factors and the determination error.

The analysis using the prediction model for Cultivar II plants showed that the 14-day sample interval had a relatively low error, with an R^2 of 0.956 and RMSEV of 0.111, and an optimum number of factors of 1. The prediction accuracy improved for plants at 6-day or longer treatments compared to 4-day or shorter day treatments and the optimum number of factors was also reduced (Table 1). At the 10-day treatment interval, the prediction model gave relatively higher errors than at 6-days or at longer treatment times; however, as in cultivar I, the optimum number of factors was reduced and the prediction model performance improved with longer periods of drought stress treatment.

Figure 3 shows the regression coefficients of the PLSR prediction models for Cultivars I and II. The figure shows representative peaks of regression coefficients derived from the results given in Table 1. The regression coefficients

Table 1. Results from the PLSR model to predict drought stress in soybean plants

Cultivar		2-day	4-day	6-day	8-day	10-day	14-day	16-day
Cultivar I (William 82)	R_c^2	0.998	0.991	0.992	0.974	0.995	0.975	0.958
	RMSEC	0.025	0.047	0.044	0.081	0.034	0.078	0.103
	R_v^2	0.95	0.973	0.958	0.97	0.989	0.963	0.95
	RMSEV	0.118	0.087	0.109	0.091	0.055	0.102	0.118
	F	10	6	7	1	4	3	1
Cultivar II (Houjaku Kuwazu)	R_c^2	0.999	0.949	0.937	0.959	0.934	0.962	0.946
	RMSEC	0.0002	0.113	0.126	0.101	0.129	0.098	0.116
	R_v^2	0.644	0.847	0.929	0.942	0.886	0.956	0.942
	RMSEV	0.316	0.207	0.141	0.128	0.179	0.111	0.127
	F	15	7	1	2	3	1	1

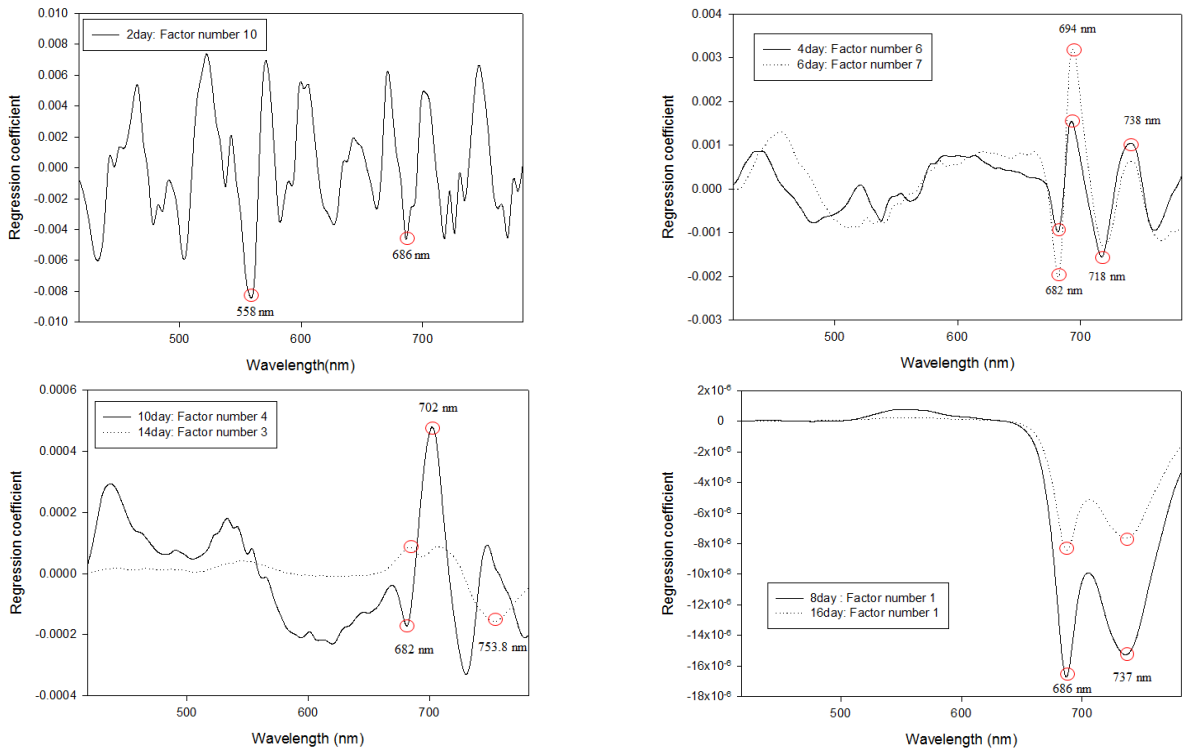

(a)

Figure 3. Regression coefficients of PLSR models for (a) Cultivar I and (b) Cultivar II.

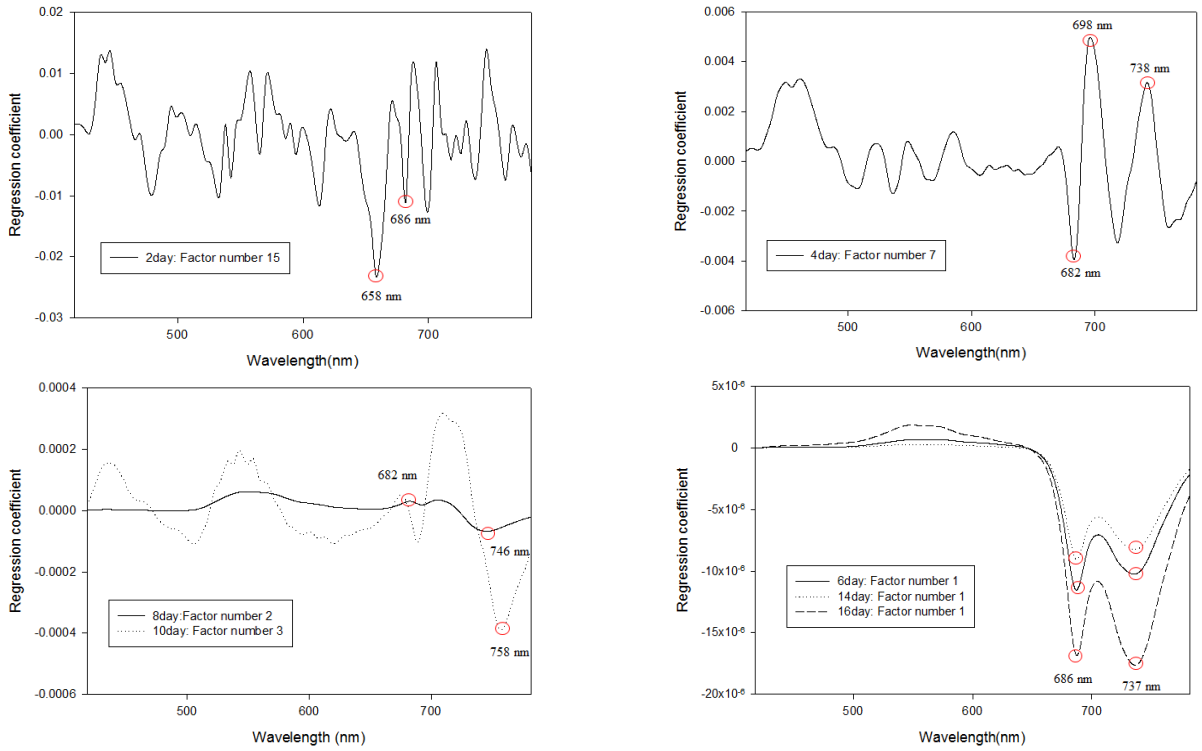

(b)

Figure 3. Regression coefficients of PLSR models for (a) Cultivar I and (b) Cultivar II (Continue).

Table 2. Representative peaks of regression coefficients in the PLSR models

	Number of optimal factor	Treatment period	Peak of regression coefficients
Cultivar I	1	8-day, 16-day	686 nm, 737 nm
	3	14-day	682 nm, 702 nm
	4	10-day	682 nm, 753 nm
	6	4-day	682 nm, 694 nm, 718 nm, 738 nm
	7	6-day	682 nm, 694 nm, 718 nm, 738 nm
	10	2-day	558 nm, 686 nm
Cultivar II	1	6-day, 14-day, 16-day	686 nm, 737 nm
	2	8-day	682 nm, 746 nm
	3	10-day	680 nm, 758 nm
	7	4-day	682 nm, 698 nm, 738 nm
	15	2-day	658 nm, 686 nm

of all models have peaks at around 686 nm or 738 nm (Table 2). These peaks are related to the wavelengths that display fluorescence characteristics of chlorophyll *a* (Gross, 1991; Buschmann et al., 1998; Gitelson et al., 1998).

Using the developed PLSR prediction model, PLS images were acquired and analyzed for the presence of drought stress (Figure 4). Table 3 presents the drought stress discrimination accuracy for each sampling interval using the pixel spectrum of the PLS images. In Cultivar I, the highest prediction accuracy occurred at the 16-day interval, and from 8-day or longer the prediction accuracy was greater than 0.964. In Cultivar II, the highest prediction accuracy was at the 14-day interval, and from 6-day, the predictive accuracy was 0.97 or higher; however, the 10-day sample had higher accuracy than that of Cultivar I. Cultivar I had 0.81 or higher accuracy at 2-day and 4-day intervals, which showed better early prediction accuracy of drought stress than that of Cultivar II. This earlier

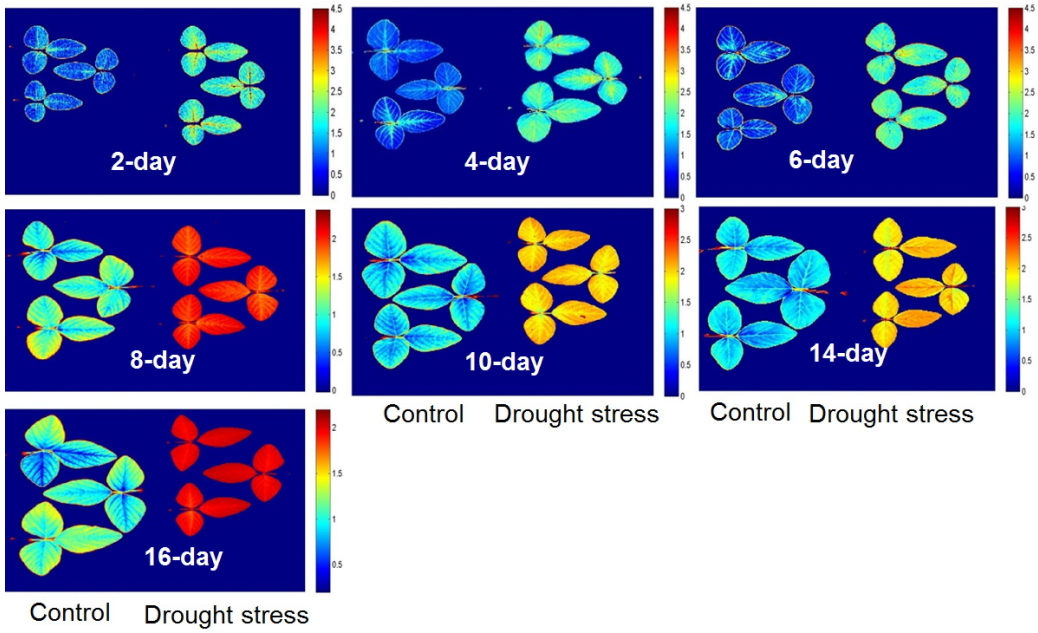

(a)

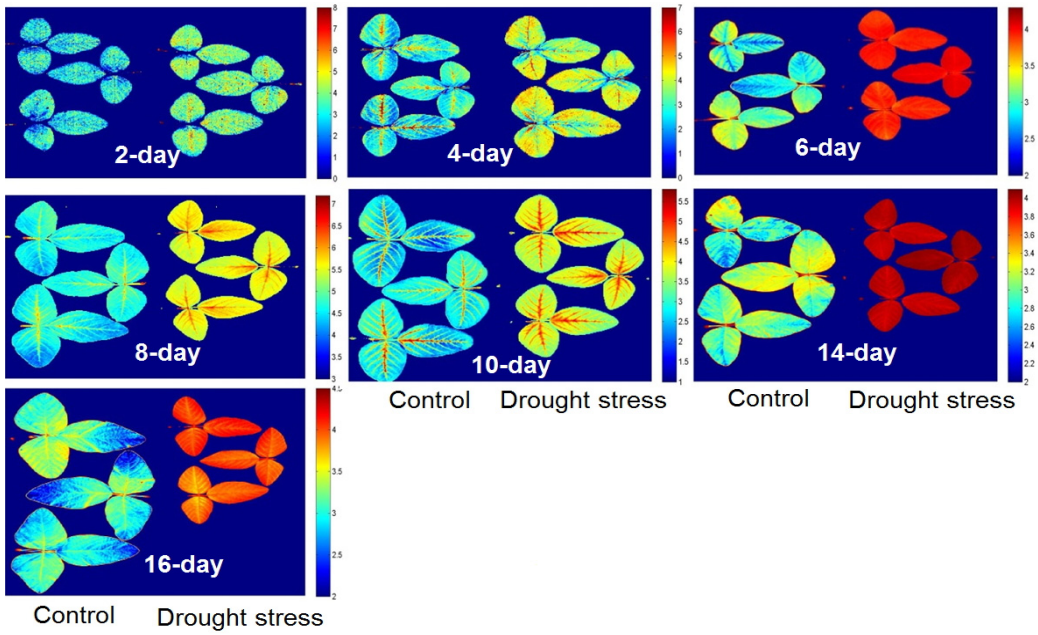

(b)

Figure 4. PLS images obtained by the PLSR model from soybean leaves of control and drought stress treated plants: (a) Cultivar I, (b) Cultivar II.

Table 3. Prediction results of drought stress in soybean plants using PLS images

Cultivar		2-day	4-day	6-day	8-day	10-day	14-day	16-day
Cultivar I (William 82)	Sensitivity	0.916	0.952	0.967	0.995	0.993	0.992	0.999
	Specificity	0.709	0.852	0.774	0.943	0.935	0.961	0.955
	Predictive accuracy	0.813	0.902	0.871	0.969	0.964	0.976	0.977
Cultivar II (Houjaku Kuwazu)	Sensitivity	0.660	0.785	0.997	0.985	0.954	0.999	0.997
	Specificity	0.737	0.757	0.950	0.955	0.836	0.970	0.963
	Predictive accuracy	0.699	0.771	0.973	0.970	0.895	0.984	0.980

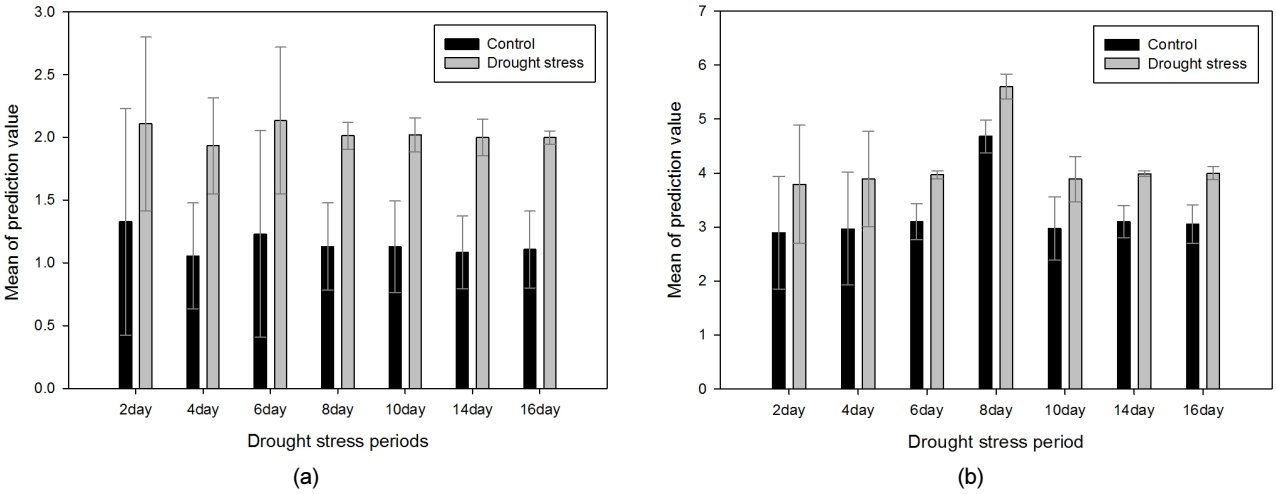

Figure 5. The mean value and standard deviation of pixel values of PLS images for control and drought stress samples at each treatment interval for the two cultivars: (a) Cultivar I, (b) Cultivar II.

prediction is attributable to higher sensitivities of Cultivar I at 2-day and 4-day, 0.916 and 0.952, respectively, as compared to Cultivar II.

The PLS image is represented by the predicted value of each pixel constituting the sample using the PLSR model. The mean values and standard deviations of all pixel values in the PLS images for each treatment period of two cultivars of soybeans are shown in Figure 5. The likely reason for the low prediction accuracy at the early stage of drought stress treatment was the low specificity in discrimination accuracy as the control group showed a large variation between pixels (Figure 5). In drought-treated plants, this variation between pixels was large up to the 6-day interval for Cultivar I and the 4-day interval for Cultivar II; the variation reduced with increased time of drought treatment. Indeed, the range of 0.048~0.146 in the drought stress treatment group at the 14-day interval was lower than the 0.289~0.357 range in the control. That is, in the early stages of drought stress, the affected part may differ depending on the position of the leaf, but as the stress period lengthened, the area of the leaf affected increased. The prediction value at the midrib of the leaf was higher than that at the tip of the leaf. Thus, drought stress in both Cultivars I and II could be discriminated within 8 days of the initiation of stress treatment by analysis of PLS images of soybean leaves.

Conclusions

In this study, a UV-A light source with an excitation wavelength of 365 nm was used to obtain hyperspectral fluorescence images to rapidly determine the presence of drought stress in soybean plants. A prediction model based on PLSR was used to indicate the presence of drought stress as it developed over a period of time in two soybean cultivars. Using the prediction model, PLS images could identify the presence of drought stress in the samples. The accuracy of drought stress discrimination in the two cultivars was 0.973 and 0.969 in the 8-day treatment group and 6-day treatment group, respectively. These results confirm the applicability of fluorescence image spectral analysis for determining drought stress in soybeans. In a future study, further samples will be used to validate the prediction model and drought stress assessment will be performed on leaves that have not been separated from the plants.

Conflicts of Interest

The authors have no conflicting financial or other interests.

Acknowledgment

This study was carried out with the support of "Research Program for Agricultural Science & Technology Development (Project No. PJ00939902)", National Institute of Agricultural Science, Rural Development Administration, Republic of Korea.

References

Buschmann, C. and H. K. Lichtenthaler. 1998. Principles and characteristics of multi-colour fluorescence imaging of plants. Journal of Plant Physiology 152:297-314.

Caires, A. R. L., M. D. Scherer, T. S. B. Santos, B. C. A. Pontim, W. L. Gavassoni and S. L. Oliveira. 2010. Water Stress Response of Conventional and Transgenic Soybean Plants Monitored by Chlorophyll a Fluorescence. Journal of Fluorescence 20:645-649.

Chang, A., J. Y. Choi, S. W. Lee, D. H. Kim and S. C. Bae. 2011. Agricultural biotechnology: Opportunities and challenges associated with climate change. Korean Journal of Plant Biotechnology 38:117-124.

Dahn, H. G., K. P. Gunther and W. Ludeker. 1992. Characterisation of drought stress of maize and wheat canopies by means of spectral resolved laser induced fluorescence. Advances in Remote Sensing 1:12-19.

Duan, L. F., W. N. Yang, C. L. Huang and Q. Liu. 2011. A novel machine-vision-based facility for the automatic evaluation of yield-related traits in rice. Plant Methods 7:44.

Gitelson, A. A., C. Buschmann and H. K. Lichtenthaler. 1998. Leaf chlorophyll fluorescence corrected for reabsorption by means of absorption and reflectance measurements. Journal of Plant Physiology 152:283-296.

Gross, J. 1991. Pigments in Vegetables: Chlorophylls and Carotenoids. New York, N.Y.: Van Nostrand Reinhold.

Houle, D., D. R. Govindaraju and S. Omholt. 2010. Phenomics: the next challenge. Nature Reviews Genetics 11(12): 855-866.

Kim, M. S., Y. R. Chen and P. M. Mehl. 2001. Hyperspectral reflectance and fluorescence imaging system for food quality and safety. Transactions of the American Society of Agricultural Engineers 44(3):721-729.

Manickavasagan, A., D. Jayas and N. White. 2008. Thermal imaging to detect infestation by cryptolestes ferrugineus inside wheat kernels. Journal of Stored Products Research 44:186-192.

Nguyen, H. T. and B. -W. Lee. 2006. Assessment of rice leaf growth and nitrogen status by hyperspectral canopy reflectance and partial least square regression. European Journal of Agronomy 24:349-356.

Rahaman, Md. M., D. Chen, Z. Gillani, C. Klukas and M. Chen. 2015. Advanced phenotyping and phenotype data analysis for the study of plant growth and development. Frontiers in Plant Science 6(619):1-15.

Rousseau, C., E. Belin, E. Bove, D. Rousseau, F. Fabre, R. Berruyer, J. Guillaumès, C. Manceau, M. A. Jacques and T. Boureau. 2013. High throughput quantitative phenotyping of plant resistance using chlorophyll fluorescence image analysis. Plant Methods 9:17.

Shibayama, M., T. Sakamoto, E. Takada, A. Inoue, K. Morita, T. Yamaguchi, W. Takahashi and A. Kimura. 2011. Regression-based models to predict rice leaf area index using biennial fixed point continuous observations of near infrared digital images. Plant Production Science 14:365-376.

Woo, N. S., M. R. Badger and B. J. Pogson. 2008. A rapid, non-invasive procedure for quantitative assessment of drought survival using chlorophyll fluorescence. Plant Methods 4:27.